

Investigation of Droplet Size Produced in Two-Phase Gravity Separators

Kul Pun, F. A. Hamad, T. Ahmed, J. O. Ugwu, J. Eyers, G. Lawson, P. A. Russell

Abstract—Determining droplet size and distribution is essential when determining the separation efficiency of a two/three-phase separator. This paper investigates the effect of liquid flow and oil pad thickness on the droplet size at the lab scale. The findings show that increasing the inlet flow rates of the oil and water results in size reduction of the droplets and increasing the thickness of the oil pad increases the size of the droplets. The data were fitted with a simple Gaussian model, and the parameters of mean, standard deviation, and amplitude were determined. Trends have been obtained for the fitted parameters as a function of the Reynolds number, which suggest a way forward to better predict the starting parameters for population models when simulating separation using CFD packages. The key parameter to predict to fix the position of the Gaussian distribution was found to be the mean droplet size.

Keywords—Two-phase separator, average bubble droplet, bubble size distribution, liquid-liquid phase.

I. INTRODUCTION

THE future of oil and gas will play an important role in world energy supply. The current global position on climate change is to reduce fossil fuel usage to reduce carbon emissions at COP26 [1]. However, the global demand for crude oil and liquid fuels is still rising [2]. Production companies have increased production to meet this demand for crude oil and natural gas. Equally, the currently used reservoirs are depleted, and enhanced techniques are required to improve recovery efficiency; therefore, the production equipment must be replaced. This involves high capital investment, and better design methods are needed to maximise profits. Oil and gas companies use three-phase separator equipment to separate phases with different densities (oil, water, and gas) from producing wells, maximising revenue and increasing supply. According to the "Global Three-phase Separator Market in the Oil and Gas Industry 2018-2022" report, the oil and gas industry will spend USD 8.9 billion on three-phase separators by 2022 [3]. Therefore, there is a need in short to medium term to improve the design of this type of apparatus.

Under previous research in this area, Teesside University [4] identified a problem with current designs design methods, including [5], [6] models. These models assume a single nominal droplet size when setting the design calculations of 500 μm , leading to wildly erroneous results when calculating actual separation efficiencies and very conservative designs. There also seemed to be a paucity of actual data that could be used to refine these calculations [4]. As a result, a need for a systematic

investigation of the effect of droplet size on separation was identified. The work presented here reports an experimental programme looking at two-phase oil-water separation. Measurements were limited to these phases because water from the oil phase controls the separation. Two variables were examined overall feed flowrate and oil layer thickness. These variables were chosen because the flow rate is thought to reduce droplet size, and the oil layer coalesce the droplets. Image processing software was used to determine droplet distributions from captured images for each experiment. The data produced were fitted with simple Gaussian models to determine if this distribution accurately represents the distribution observed.

II. LITERATURE REVIEW

The diameter, volume, and number density of fluid particles, as well as the size and distribution of droplets within the continuous phase, have a significant impact on the exchange of mass, momentum, and energy between dispersed phased liquid drops and continuous phased liquid flow from a physical standpoint [7]. This explains why [8] found that droplet diameter is a significant factor in determining the separation performance of multiphase gravity separators. Their findings were backed up by [9] which stated that "droplet diameter has been the leading primary cause of the gap between experimental and CFD results". As a result, several researchers [4], [6], [10]-[14] have made assumptions about droplet size distribution for their experiments.

Given this accepted dependence of separator performance on droplet size, there has been little published effort to examine this experimentally. The only known experimental work for three-phase separators is described below:

Reference [15] proposed a method for sizing three-phase separators using a droplet size distribution. They tested their method using a three-phase separator with a diameter of 4420 mm and an overall length of 15850 mm and using the Sauters-Brown equation with an appropriate k factor for gas-liquid separation and an actual retention time obtained from lab and field experiments to find the liquid-liquid separation. The results confirmed that oil and water droplets of more than 90 μm would separate from the gas. The water droplets smaller than 225 μm would be lost in the oil outlet with 4.5% separation efficiency. The oil droplets smaller than 60 μm would be lost in the water outlet of the three-phase separator.

Reference [4] used ANSYS Fluent to simulate a three-phase separator with a diameter of 300 mm and a length of 900 mm

Kul Pun is with Teesside University, United Kingdom (corresponding author, e-mail: k.pun@tees.ac.uk).

using the turbulence model combined with the volume of fluid (VOF) and Eulerian models to see if they could increase agreement between simulation and experimental results by changing the mean bubble droplets. They used the following six droplet diameters: 100 μm , 200 μm , 350 μm , 500 μm , 750 μm and 1000 μm . They found that low flows CFD predictions using 500 μm underestimated the experimental results by 10% for separation in the oil phase. Changing the droplet size did not affect the agreement. However, at high flows, where it would be expected that the droplets have reduced in size, they discovered that the CFD overestimated the separation by 15% for 500 μm particles. When they reduced the diameter to 350 μm , they improved agreement to 1.5%. They concluded that the model is very dependent on mean droplet size and some way needs to be found to link flow rate to droplet size to improve design simulations.

Aside from this, many CFD studies have been performed [4], [14] and [19] to find droplet diameter distributions, but the

literature review revealed that little work [15] had been done to confirm their distributions with actual separator bubble distribution data.

III. EXPERIMENTAL SET UP

A variable geometry experimental apparatus was developed at Teesside University to investigate the effect of the L/D ratio on separator performance by [4]. This apparatus has been modified to allow the measurement of droplet size.

A. Overview of the Experimental Test-Rig

The Teesside University Horizontal Three-Phase Separator (HTPS) is made from transparent polypropylene, allowing visual observation of the separator's flow regimes. It has a fixed diameter of 300 mm and a length range of 600 mm to 1500 mm, giving an adjustable L/D ratio of 2:1 to 7:1. Fig. 1 shows the Piping and Instrument Diagram (P&ID).

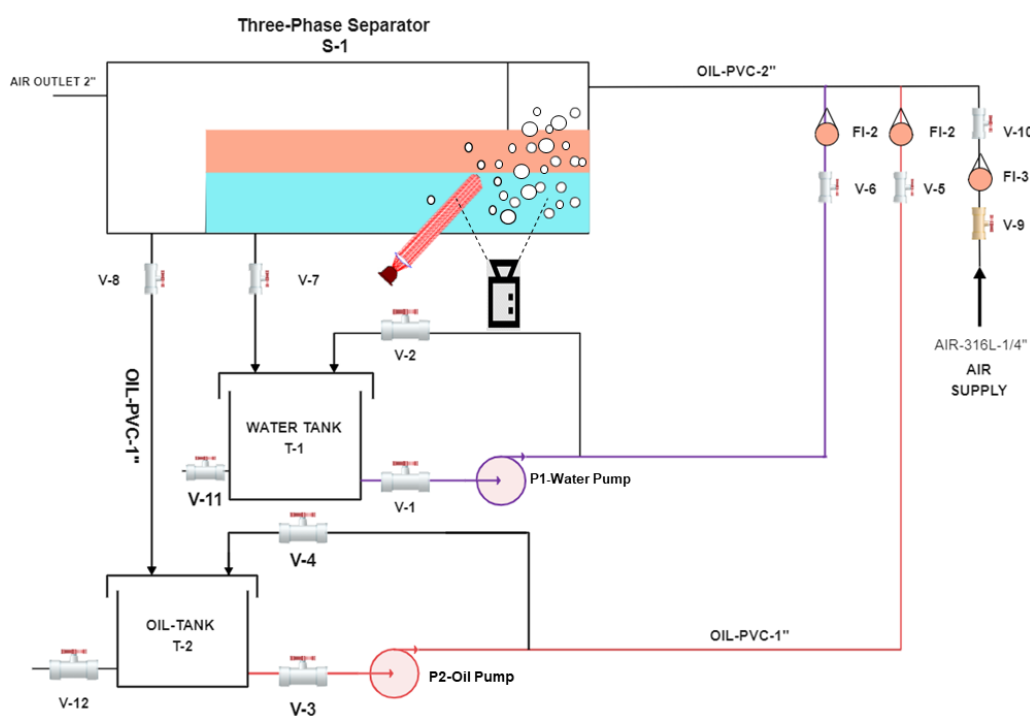


Fig. 1 Schematic diagram of the experiment set-up: (P1 and P2) Water and oil centrifuge pump, (V1 to V12) Control ball valve, (F1, F2 and F3) Rotameters flow meters, (S-1) Three-phase separator, and (T1 and T2) Water and oil tank, camera, and light

The apparatus has been modified to measure the droplet distribution. Measurements are made in the separator body and not in the inlet pipe because the inlet geometry can modify the droplet size distribution.

The apparatus has been fitted with light below the inlet deflector. A high-speed camera is mounted at right angles to the separator to capture the oil droplets rising through the water layer.

B. Experimental Methods and Procedures

This experimental programme aimed to determine the droplet size distribution for a given set of flow measurements.

A typical experiment would start with an empty separator, all valves shut, and the pumps switched off. Return valves in the kickback lines are opened halfway, as are the discharge valves V5 and V6. The pump inlet valves are then opened to allow fluid to move into the pumps and prime them under the static head from the feed tanks. The pumps are then started, and the kickback valves and discharge valves are adjusted to give the desired flow rates. Usually, the system is set to operate at the lowest measurable flow. The liquid level rises slowly in the separator and establishes an oil pad on top of the water layer. The water liquid level is controlled by adjusting the ball valve V-7. During operation, this was utilised to change the height of

the oil-water interface. The oil builds up and overflows on a fixed height weir set to run at the centreline of the separator. Adjusting ball valve V-8 controls the outlet flow rate of oil downstream of the weir. The apparatus is run for 15 minutes at a steady state to establish the initial steady-state concentrations of the phase. Once a steady-state was established, photographs of the droplet distribution were taken. A video of the droplet flow was recorded simultaneously to consider the dynamic droplet behaviour if problems were encountered when analysing the photographic data. Experiments were carried out in a random pattern to avoid establishing hysteresis.

Finally, the oil flow stops, the pump shuts down, and the oil-water interface rises until the interface reaches the top of the weir. The water valve V-8 is then opened fully, and the water pump is shut down, allowing the water to drain back into its feed tank. Water entrained in the oil outlet can settle in T-2 and remove V-12. Oil entrained in water is skimmed from tank T-1 and returned to the oil tank.

C. Image Capture Measurement to Determine Droplet Size

After steady-state was established, the droplet distribution of oil and water was captured using a SONY Alpha 7 (III) camera with a 28-70 mm zoom lens by observing the rising motions of bubbles at the viewing section of the separator inlet and capturing them as still images. The fluid was illuminated using a 100 W LED studio lite panel light mounted perpendicular to the camera. The parameters of the high-speed camera were set as follows: resolution 1920 x 1080, frame rate 500 f/s and record-setting of 50P 50M, which provided the largest viewing area. For better visualisation, the camera has been accurately

aligned horizontally and located 100 mm from the test rig. To reduce errors, working distance, focal length, and field depth were fixed and checked in every experiment.

The oil-water's two phases' recorded images were stored in a personal computer and processed using image analysis software. The recorded frames were examined and selected carefully. Calibration of the camera images was necessary to convert the still image captured as pixels into actual metric dimensions [16]. A single drop of known dimensions was photographed under the same conditions as the actual measurement and used to obtain a relationship between pixels and mm. Each image was magnified by a factor of five to give the desired resolution. Each pixel was found to represent an actual distance of 53 μm . Reference [15] stated that droplets less than 60 μm would be lost in the water phase anyway, and the normal starting diameter is assumed to be 500 μm . This represents an acceptable accuracy of detection for the droplets of interest.

D. Image Analysis Processing

The next step was to develop a standard method to analyse the photographs and the derived droplet data. This is described as: The bubble diameter distributions captured by the camera were extracted using an image analysis tool (Image J). Image J is a freeware java-based image processing programme that is faster and more accurate than sieve analysis [17]. This tool has been used in various applications, including biomedical, powder technology, and food processing, and can evaluate various size and shape criteria [17]. The steps involved in image processing are shown schematically in Fig. 2.

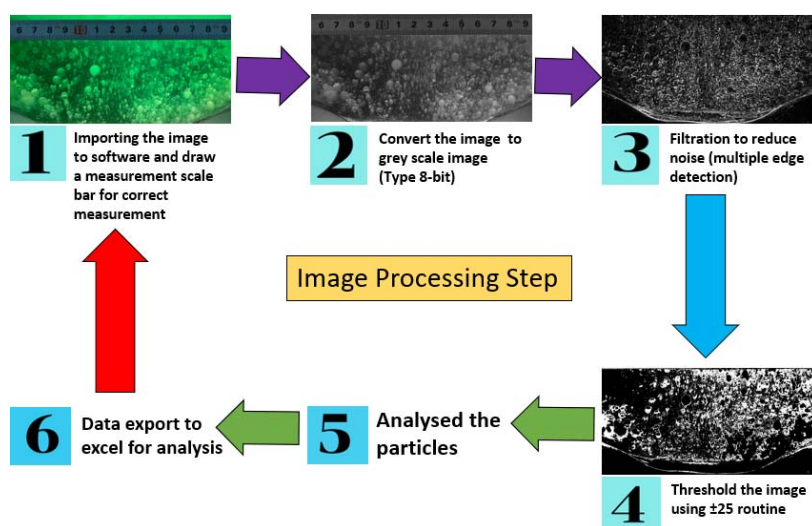


Fig. 2 Flow diagram of particle droplet dimension measurement using image J

In Fig. 2, Step 1 involves taking the camera's colour image and converting it to an 8-bit grayscale image. If the image is over-illuminated, the lighting is adjusted by subtracting the background lighting level [18]. The threshold value for the normalised image is then applied in step 2. The contours that are now highlighted correctly approximate real-world interface locations because maximum grey level intensity gradients may

be determined. Step 3 converts the image into a pure binary black and white image. This conversion is achieved by applying a global threshold. Binarised processing contains several processes to minimise image noise while maintaining the structure of binary objects: area opening, median filtering, thinning, thickening, picture filling, and skeletonisation [20]. In step 4, the image of the round item was detected using the

circular Hough transform [21]. The circular object bubbles were then extracted using the multi-edge detection approach [22]. The next step uses the calibration data from the measured single droplet to scale the image. The software then converts the extracted bubbles into sized images and counts the droplets in given ranges.

E. Post Image Processing of the Numerical Droplet Distributions

After image processing, the image software produces an output that lists droplet counts and their specific areas (μm^2). These were then processed in MS Excel to determine the radius and diameter of the droplet in each category in μm . The list of diameter categories is over 20,000, which is too large to analyse sensibly, but many of the categories are repeated. Therefore, the categories with common diameters were added together to give the actual total count of droplets with a given diameter. These data are shown as a plot of the mean bubble diameter versus the number of bubble droplets in Fig. 3.

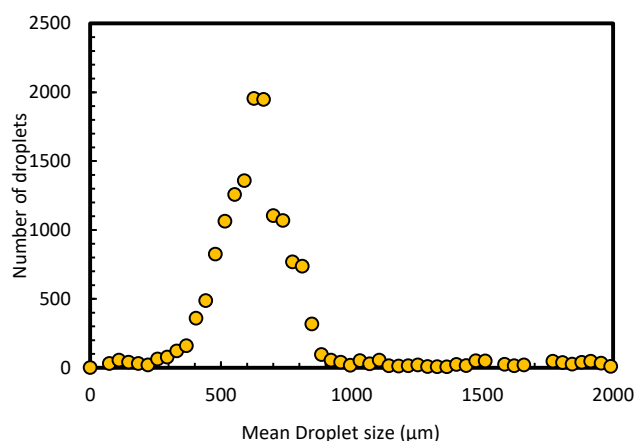


Fig. 3 Experimental result of bubble droplet versus the number of droplets from sample data

IV. EXPERIMENTAL RESULTS

It was decided to set up the experiment for nominal total flows of equal flows in gallons per minute of water and oil using the rotameters on the apparatus to cover the full range of experiments. Four different flows rate and four different oil pad thicknesses were set. The data collected for this group of experiments were recorded, and these data are fitted with the Gaussian curve.

Figs. 4 (a) and (b) show the bubble size distribution. As the bulk flow increases, the droplet means diameter decreases. Equally, as the layer thickness increases, the spread of the peaks increases indicating an increase in the particle size range. The mean diameter observed to move to the size of the right increases. This is thought to be due to the increasing power to coalesce the droplets as they pass through the oil pad.

A. Fitted Parameters for the Gaussian Model

The same three parameters were plotted as functions of Reynolds number in Figs. 5 (a)-(c) for the different oil layer thicknesses. Linear fits of the data points represented the data

well.

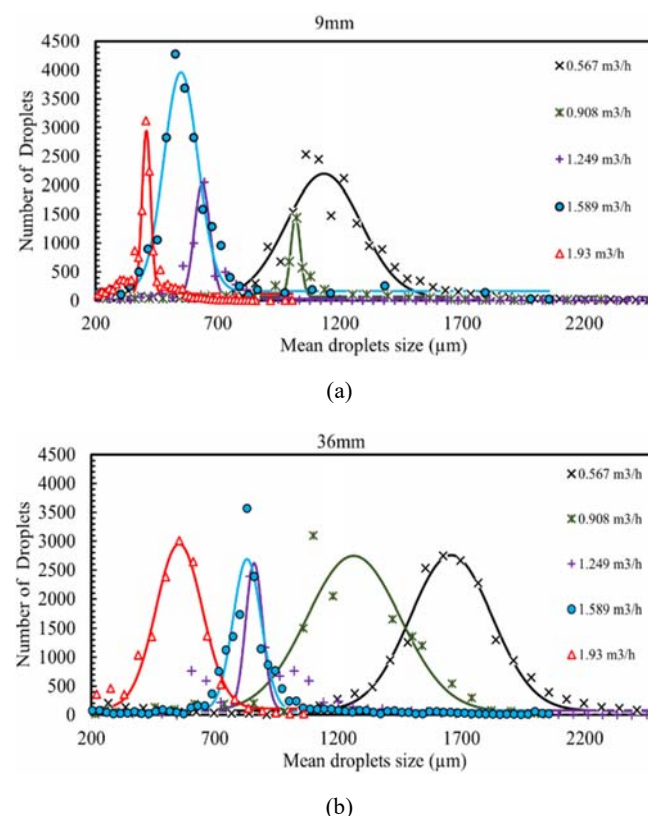


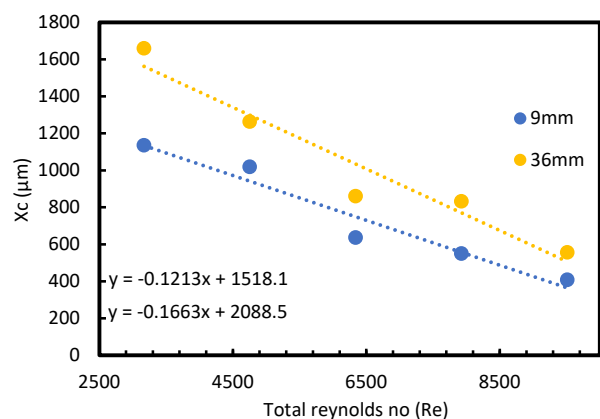
Fig. 4 Plot of the number of bubble droplets with various mean bubble droplet sizes: (a) 9 mm and (b) 36 mm

V. CONCLUSIONS

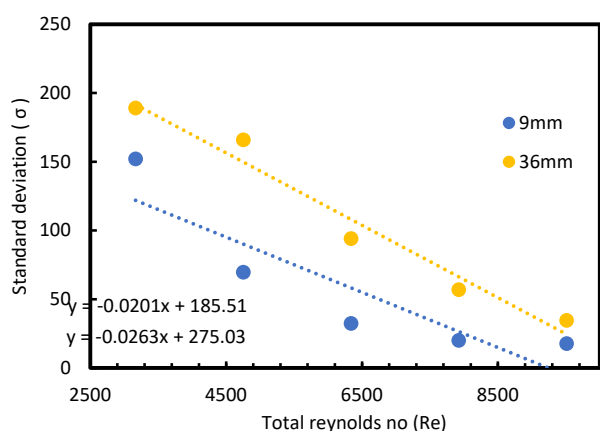
In this study, Particle Image Velocimetry (PIV) measurement techniques were used to successfully record bubble size distributions of water in oil droplets created in a two-phase separator.

Data measured using this technique investigated the different parameters affecting droplet sizes. As expected, droplet size was found to reduce as a function of bulk flow, but increased oil pad layer thickness increases droplet coalescence, increasing mean droplet size and the spread of droplet sizes.

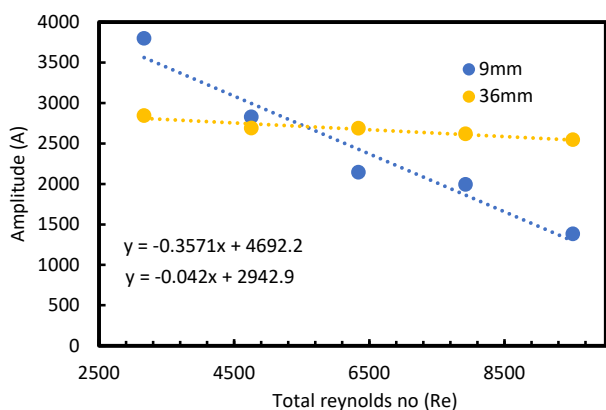
It was found that the droplet size distribution could be represented well using a simple Gaussian distribution. Further, it was found that the mean droplet size, standard deviation, and amplitude of the droplets all vary systematically and can be represented by simple straight-line relationships. This gives a straightforward way to predict the droplet size distribution for a separator simulation if the mean droplet size for a given inlet flow can be found.



(a)



(b)



(c)

Fig. 5 Plots of three primary variables against total Reynolds numbers: (a) mean droplet size x_c , (b) standard deviation σ and (c) peak amplitude A at 0.25:0.75 volume of a fraction

REFERENCES

[1] Asselt, H. van (2021) Breaking a Taboo: Fossil Fuels at COP26, Breaking a Taboo: Fossil Fuels at COP26 – EJIL: Talk! www.ejiltalk.org. Available at: <https://www.ejiltalk.org/breaking-a-taboo-fossil-fuels-at-cop26/> (Accessed: April 5, 2022)

[2] Short-Term Energy Outlook. (2022) Washington, D.C: Energy Information Administration, Office of Energy Markets and End Use, U.S. Dept. of Energy. Available at: https://www.eia.gov/outlooks/steo/report/global_oil.php (Accessed: April 6, 2022)

[3] Wood, L. (2018) Global Three-phase Separator Market in the Oil and Gas Industry 2018-2022 - ResearchAndMarkets.com Available at: <https://www.businesswire.com/news/home/20180807005429/en/Global-Three-phase-Separator-Market-in-the-Oil-and-Gas-Industry-2018-2022-ResearchAndMarkets.com> (Accessed: April 5, 2022).

[4] Ahmed, T. G. (2021) Optimisation of three-phase separator design through computational fluid dynamics simulation and experimental investigation. Teesside University.

[5] Monnery, W. and Svrcek, W. (1994) 'Successfully Specify Three-Phase Separators', Chemical Engineering Progress, 90(9), pp. 29–40

[6] Stewart, M. and Arnold, K.E (2008). Surface Production Operations. Volume 1, Design of Oil Handling Systems and Facilities.

[7] Yeoh, G. H. and Tu, J. (2014) Multiphase Flow Analysis Using Population Balance Modeling. Multiphase Flow Analysis Using Population Balance Modeling. doi: 10.1016/c2011-0-05568-0.

[8] Ahmed, T., Hamad, F. and Russell, P. A. (2017) 'The use of CFD simulations to compare and evaluate different sizing algorithms for three-phase separators', OTC Brasil 2017, pp. 1051–1066. DOI: 10.4043/28066-ms.

[9] Kharoua, N., Khezzer, L. and Saadawi, H. (2012) 'Using CFD to model the performance of retrofit production separators in Abu Dhabi', Society of Petroleum Engineers - Abu Dhabi International Petroleum Exhibition and Conference 2012, ADIPEC 2012 - Sustainable Energy Growth: People, Responsibility, and Innovation, 3, pp. 1776-1784. doi: 10.2118/161521-ms.

[10] Wright, c. c. & Douglas, D. w., 1966. The disposal of APA oil field wastewater. American petroleum institute

[11] Hopper, w. b. & Jacobs, L., 1996. Handbook of Separation Techniques for Chemical Engineers. 3 ed. s.l.:s.n.

[12] Pourahmadi Laleh, A., 2010. CFD simulation of multiphase separators, Calgary: University of Calgary-doctoral thesis.

[13] Walas, M. & Stanley, 1990. Chemical Process, Equipment Selection and Design. USA: USA inc.

[14] Oshinowo, L. M. and Vilagines, R. D. (2020) 'Modeling of oil-water separation efficiency in three-phase separators: Effect of emulsion rheology and droplet size distribution', Chemical Engineering Research and Design, 159, pp. 278–290. DOI: 10.1016/j.cherd.2020.02.022

[15] Song, J. H. et al. (2010) 'Three-phases separator sizing using drop size distribution', Proceedings of the Annual Offshore Technology Conference, 2(May), pp. 1011–1023. DOI: 10.4043/20558-ms.

[16] Zhai, L. S. et al. (2017) 'Measurement of droplet sizes in bubbly oil-in-water flows using a fluid-sampling device', Measurement: Journal of the International Measurement Confederation, 102, pp. 296–308. doi: 10.1016/j.measurement.2017.01.055.

[17] Rishi Kumari and Narinder Rana (2015) 'Particle Size and Shape Analysis using ImageJ with Customised Tools for Segmentation of Particles', International Journal of Engineering Research and, V4(11), pp. 247–250. DOI: 10.17577/ijertv4is110211.

[18] Laupsien, D., Le Men, C., Cockx, A. and Liné, A., 2019. Image processing for bubble morphology characteristics in diluted bubble swarms. Physics of Fluids, 31(5), p.053306.doi: 10.1063/1.5088945

[19] Liang, Y., Zhao, S., Jiang, X., Jia, X. & Li, W. 2013, "Numerical simulation on flow field of oilfield three-phase separator", Journal of Applied Mathematics, vol. 2013.

[20] Wilson, D.A., Pun, K., Ganesan, P.B. and Hamad, F. (2021b) 'Geometrical optimisation of a venturi-type microbubble generator using CFD simulation and experimental measurements', Designs, 5(1), pp. 1–18. doi: 10.3390/designs5010004

[21] Lappalainen, T. and Lehmonen, J. (2012) 'Determinations of bubble size distribution of foam-fibre mixture using circular hough transform', Nordic Pulp and Paper Research Journal, 27(5), pp. 930–939. doi: 10.3183/NPPRJ-2012-27-05-p930-939

[22] Guo, F., Yang, Y., Chen, B. and Guo, L. (2010) 'A novel multi-scale edge detection technique based on wavelet analysis with application in multiphase flows', Powder Technology, 202(1-3), pp. 171-177